Nano Research
DOI 10.1007/s12274-017-1657-5
Research Article
ISSN 1998-0124
CN 11-5974/O4

High-performance aqueous symmetric sodium-ion battery using NASICON-structured $Na_2VTi(PO_4)_3$

Hongbo Wang[1], Tianran Zhang[2], Chao Chen[3], Min Ling[4], Zhan Lin[1,3] (✉), Shanqing Zhang[4], Feng Pan[5], and Chengdu Liang[1]

[1] *Zhejiang Provincial Key Laboratory of Advanced Chemical Engineering Manufacture Technology, College of Chemical and Biological Engineering, Zhejiang University, Hangzhou 310027, China*
[2] *Department of Mechanical Engineering, National University of Singapore, Singapore 117576, Singapore*
[3] *College of Light Industry and Chemical Engineering, Guangdong University of Technology, Guangzhou 510006, China*
[4] *Centre for Clean Environment and Energy, Environmental Futures Research Institute and Griffith School of Environment, Gold Coast Campus, Griffith University, QLD 4222, Australia*
[5] *School of Advanced Materials, Peking University, Shenzhen Graduate School, Shenzhen 518055, China*

Received: 26 February 2017
Revised: 25 April 2017
Accepted: 30 April 2017

KEYWORDS
$Na_2VTi(PO_4)_3$,
aqueous,
symmetric,
sodium-ion batteries

ABSTRACT

A high-safety and low-cost route is important in the development of sodium-ion batteries, especially for large-scale stationary battery systems. An aqueous sodium-ion battery is demonstrated using a single NASICON-structured $Na_2VTi(PO_4)_3$ material with the redox couples of V^{4+}/V^{3+} and Ti^{4+}/Ti^{3+} working on the cathode and anode, respectively. The symmetric full cell fabricated based on the bi-functional electrode material exhibits a well-defined voltage plateau at ~1.2 V and an impressive cycling stability with capacity retention of 70% exceeding 1,000 cycles at 10C (1C = 62 mA·g^{-1}). This study provides a feasible strategy for obtaining high-safety and low-cost rechargeable batteries using a single active material in aqueous media.

1 Introduction

Mobile electronic devices require rechargeable batteries exhibiting high energy and power densities, and lithium-ion batteries (LIBs) have been widely commercialized for this purpose [1, 2]. However, the relatively high cost of LIBs has prevented their use in further applications in stationary power stations. Sodium-ion batteries (NIBs) are potential alternatives to LIBs for use in stationary energy storage systems because of the abundance of natural sodium sources with a low cost [3, 4]. Furthermore, symmetric NIBs are promising from a commercial standpoint as the same active material can be used as both the cathode and anode. This bi-functional material simplifies the electrode design and reduces the manufacturing cost

Address correspondence to zhanlin@zju.edu.cn

as a single powder preparation and slurry casting process can be employed for fabricating the positive and negative electrodes in NIBs [5–8].

For developing symmetric NIBs, an electrode material that serves both as a sodium-rich cathode and sodium-deficient anode is required, e.g., layered metal oxides, such as P2-$Na_{0.6}Cr_{0.6}Ti_{0.4}O_2$ and O3-$Na_{0.8}Ni_{0.4}Ti_{0.6}O_2$, that were successfully used in non-aqueous electrolytes [9, 10]. However, non-aqueous electrolytes are inflammable; and the cycling performances of currently developed symmetric NIBs in non-aqueous electrolytes are insufficient for use in long-term operations in stationary electrical energy storage requiring high safety. As compared with non-aqueous electrolytes, the use of NIBs exhibiting a much higher safety and lower cost in aqueous electrolytes is a promising approach for achieving large-scale electrical energy storage for stationary applications [11–13]. However, both the positive and negative electrodes in aqueous NIBs should function within the electrochemical potential windows of water [14, 15]. Thus, it is greatly significant and challenging to search for a suitable bi-functional material to fabricate aqueous symmetric NIBs exhibiting a long cycle life for applications in high-performance stationary power stations.

As well known, the redox potentials of vanadium (V) and titanium (Ti) present in NASICON-structured compounds are within the electrochemical potential window of water [16]. NASICON-structured $Na_3V_2(PO_4)_3$ is believed to be a promising cathode material, while the isostructural $NaTi_2(PO_4)_3$ served as a good anode material in aqueous NIBs [17–20]. However, V-based phosphate cathode materials degrade easily in commonly used aqueous electrolytes [21–23], which can be stabilized by substituting half of the V sites with Ti for applications in aqueous media. Herein, we synthesized NASICON-structured $Na_2VTi(PO_4)_3$ that served as not only as the cathode but also as the anode to construct a symmetric NIB in aqueous electrolyte. The resultant symmetric cell exhibits a voltage of ca. 1.2 V with an initial discharge capacity of 50 $mAh \cdot g^{-1}$ at a rate of 1C (1C = 62 $mA \cdot g^{-1}$), corresponding to 80.3% of the theoretical maximum capacity (62 $mAh \cdot g^{-1}$). The important properties required for stationary batteries to be used in large-scale electrical energy storage are long life, high safety, and low cost, which are more important than specific energy [24, 25]. The resulting symmetric NIB exhibits an energy density of ~30 $Wh \cdot kg^{-1}$ with a superior long life, i.e., exceeding 1,000 cycles with a capacity retention of 70% even at a high current rate of 10C, making it a promising rechargeable battery for stationary power stations.

2 Experimental

2.1 Material preparations

$Na_2VTi(PO_4)_3$ was prepared using CH_3COONa, NH_4VO_3, $(CH_3CH_2CH_2CH_2O)_4Ti$, and $NH_4H_2PO_4$ as the raw materials. Citric acid was employed as both a chelating agent and a carbon source, which reduces V^{5+} to V^{3+}. Initially, CH_3COONa, NH_4VO_3, $NH_4H_2PO_4$, and citric acid with stoichiometric ratios were dissolved in distilled water with magnetic stirring. After using acetic acid to adjust the pH of the above solution to 4.0, a diluted solution of $(CH_3CH_2CH_2CH_2O)_4Ti$ in ethanol was poured into the solution to achieve the final stoichiometry under vigorous stirring. The obtained mixture was evaporated at 80 °C in a water bath to form a uniform sol and further dried in an oven at 120 °C overnight to obtain a gel precursor. This gel precursor was sintered at 450 °C under argon flow for 3 h followed by 850 °C for 12 h. The resultant material was pulverized and sieved by ~300 meshes for performing the electrochemical and structural studies.

2.2 Material characterizations

Powder X-ray diffraction (XRD) analysis was performed on a PANalytical Empyrean200895 with Cu Kα radiation. The XRD data was refined using the GSAS Rietveld software, and the electrodes obtained by dissembling batteries cycled at various voltages were characterized using *ex-situ* XRD. Transmission electron microscopy (TEM) and scanning electron microscopy (SEM) measurements were performed on JEOL JEM2100 and FEI SIRION100 microscopes equipped with energy dispersive X-ray spectroscopy (EDS) for performing elemental analysis, respectively. X-ray photoelectron spectroscopy (XPS) measurements were performed on a ThermoFisher Escalab250Xi equipment. Raman spectra were recorded on a Horiba LabRAM HR microscope using 532 nm excitation.

Thermal gravimetric analysis (TGA) was carried out on a Mettler TA Q500 instrument at a heating rate of 10 °C·min^{-1} under air atmosphere.

2.3 Electrochemical measurements

The working electrode was prepared by rolling a mixture of 70 wt.% $Na_2VTi(PO_4)_3$, 20 wt.% carbon black, and 10 wt.% polytetrafluoroethylene (PTFE) into a thin film, followed cutting it into a circular strip of 8 mm in diameter and pressing the strip (ca. 4.5 mg) onto a Ti mesh. The electrode was used in a three-electrode system with 1.0 mol·L^{-1} Na_2SO_4 as the aqueous electrolyte, $Na_2VTi(PO_4)_3$ as the working electrode, activated carbon as the counter electrode, and the Ag/AgCl electrode saturated with KCl (0.197 V vs. NHE) as the reference electrode. The symmetric aqueous cell fabricated with $Na_2VTi(PO_4)_3$ as the cathode and the anode was assembled in a 2025-type coin cell using glass fiber as the separator. The weight ratio of the anode to the cathode in the cell was ~1.10. The specific capacity of the half-cell in the three-electrode system was calculated using the mass of the active material of $Na_2VTi(PO_4)_3$, while the specific capacity of the symmetric full-cell was calculated based on the mass of the corresponding active material in the positive electrode. Cyclic voltammetry (CV) and linear sweep voltammetry tests were carried out on a CHI760D electrochemical workstation at a scan rate of 0.5 mV·s^{-1}. Galvanostatic charge and discharge measurements were conducted on a LAND battery testing system at various rates at room temperature.

3 Results and discussion

The crystal structure of $Na_2VTi(PO_4)_3$ was characterized using XRD, as shown in Fig. 1. The diffraction pattern clearly shows the presence of a single phase, and no crystalline impurities are observed. All the diffraction peaks indicate that $Na_2VTi(PO_4)_3$ crystallizes in the rhombohedral NASICON structure with a space group of $R\bar{3}c$, and the peaks are sharp and well defined, demonstrating a good crystallinity. The refined profiles fitted well with the experimental data, and the unit cell parameters obtained from the structural refinement are a = 8.6031(6) Å and c = 21.8245(16) Å (Table S1 in the Electronic Supplementary Material (ESM)). The

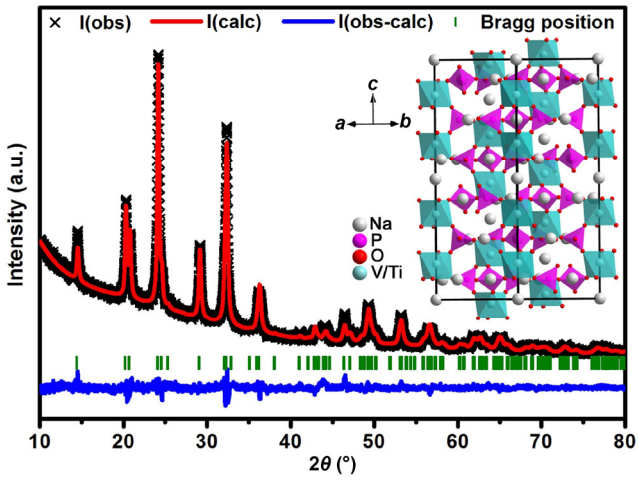

Figure 1 XRD pattern of $Na_2VTi(PO_4)_3$ and Rietveld refinement. The inset schematically represents the crystal structure of $Na_2VTi(PO_4)_3$.

schematic illustration of the NASICON unit cell of $Na_2VTi(PO_4)_3$ is represented in the inset of Fig. 1, in which the isolated VO_6 or TiO_6 octahedra shares all of its corners with PO_4 tetrahedra, forming a three-dimensional (3D) framework. Two different types of sodium ions are located in the interstitial sites of the framework with two different oxygen environments: A single interstitial site per unit cell with a six-fold coordination (Na_1 site) is occupied by a less mobile sodium-ion, while two equivalent sites per unit cell with an eight-fold coordination (Na_2 sites) are occupied by a mobile sodium-ion. Sodium ions positioned at the Na_2 sites can be extracted/inserted for the electrochemical activity [26]. As a result, one sodium ion per unit cell is extracted from $Na_2VTi(PO_4)_3$ with the formation of $NaVTi(PO_4)_3$ through the V^{4+}/V^{3+} redox couple, while another sodium ion per unit cell is inserted into $Na_2VTi(PO_4)_3$ with the formation of $Na_3VTi(PO_4)_3$ through the Ti^{4+}/Ti^{3+} redox couple.

The morphologies of $Na_2VTi(PO_4)_3$ were investigated via SEM and TEM. As shown in Figs. 2(a) and 2(b), the $Na_2VTi(PO_4)_3$ powder is composed of agglomerate particles having sizes of hundreds of nanometers. The high-magnification TEM image reveals that a uniform carbon layer with a thickness of ca. 7 nm is coated on the surface of the $Na_2VTi(PO_4)_3$ particles (Fig. 2(c)). Inside the nanoparticles, clear lattice fringes with spacing of 0.367 and 0.593 nm, corresponding to the interplanar spacing of (113) and (012) planes

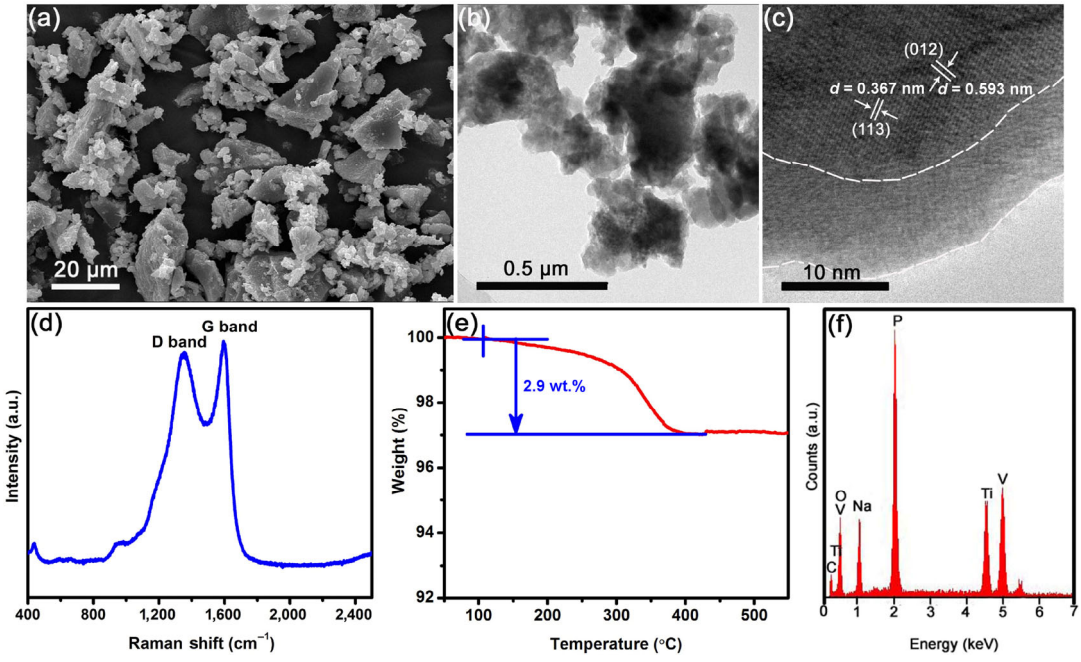

Figure 2 Characterizations of the $Na_2VTi(PO_4)_3$ material. (a)–(c) SEM, TEM, and HRTEM images. (d) Raman spectrum. (e) and (f) TGA and EDS analysis.

of the rhombohedral structure, are observed. The existence of the carbon layer was also confirmed from the Raman spectrum. As shown in Fig. 2(d), the group of peaks observed at 1,594 and 1,354 cm^{-1} can be assigned to the graphite band (G band) and the disorder-induced phonon mode (D band) of carbonaceous materials, respectively. Furthermore, the characteristic peaks of $Na_2VTi(PO_4)_3$ were observed at 960 and 436 cm^{-1} [27, 28]. The amount of carbon was estimated to be ca. 2.9 wt.% from the weight loss in the TGA, as shown in Fig. 2(e); and the presence of carbon improves the electrical conductivity of the material. Hence, the $Na_2VTi(PO_4)_3$ material is expected to exhibit a superior rate capability. We conducted EDS measurements by pressing the $Na_2VTi(PO_4)_3$ material into a pellet. The elements Na, V, Ti, P, O, and C are observed in the EDS image as shown in Fig. 2(f), and the atomic ratios of Na, V, Ti, and P are close to the stoichiometric ratios of the $Na_2VTi(PO_4)_3$ lattice (Table S2 in the ESM).

Electrochemical properties of the $Na_2VTi(PO_4)_3$ electrode on using as a cathode were characterized by CV and galvanostatic charge/discharge tests performed in a three electrode system with Ag/AgCl as the reference electrode in aqueous Na_2SO_4 electrolyte. As shown in Fig. 3(a), a pair of symmetric redox peaks appears at ~0.42 V vs. Ag/AgCl and remains unchanged during successive scans, suggesting the cycling stability of the $Na_2VTi(PO_4)_3$ material in aqueous Na_2SO_4 solution. Based on the intercalation chemistry of V-based phosphate compounds [21, 29], this pair of redox peaks is attributed to the reversible reaction of the V^{4+}/V^{3+} couple in the $Na_2VTi(PO_4)_3$ lattice as in Eq. (1):

$$Na_2VTi(PO_4)_3 - xNa^+ - xe^- \rightleftharpoons Na_{2-x}VTi(PO_4)_3 \quad (1)$$

We theoretically defined 62 $mA{\cdot}g^{-1}$ as 1C, which corresponds to the complete discharge of the $Na_2VTi(PO_4)_3$ electrode in 1 h. Fig. 3(b) shows the cycling performance of the $Na_2VTi(PO_4)_3$ electrode achieved in the first five cycles at 1C. The initial charge/discharge capacities are 58 and 56 $mAh{\cdot}g^{-1}$, respectively, corresponding to a high Coulombic efficiency of ~97%. During the first charge/discharge, V^{3+} oxidizes to V^{4+} on charging and V^{4+} reduces to V^{3+} on discharging, while the valence state of Ti^{4+} is unchanged (Fig. S1 in the ESM). All the XRD peaks of $Na_2VTi(PO_4)_3$ shift to higher angles on charging to 0.6 V, indicating volume shrinkage occurring owing to the extraction of sodium ions from the NASICON structure [30], and the diffraction peaks of the electrode

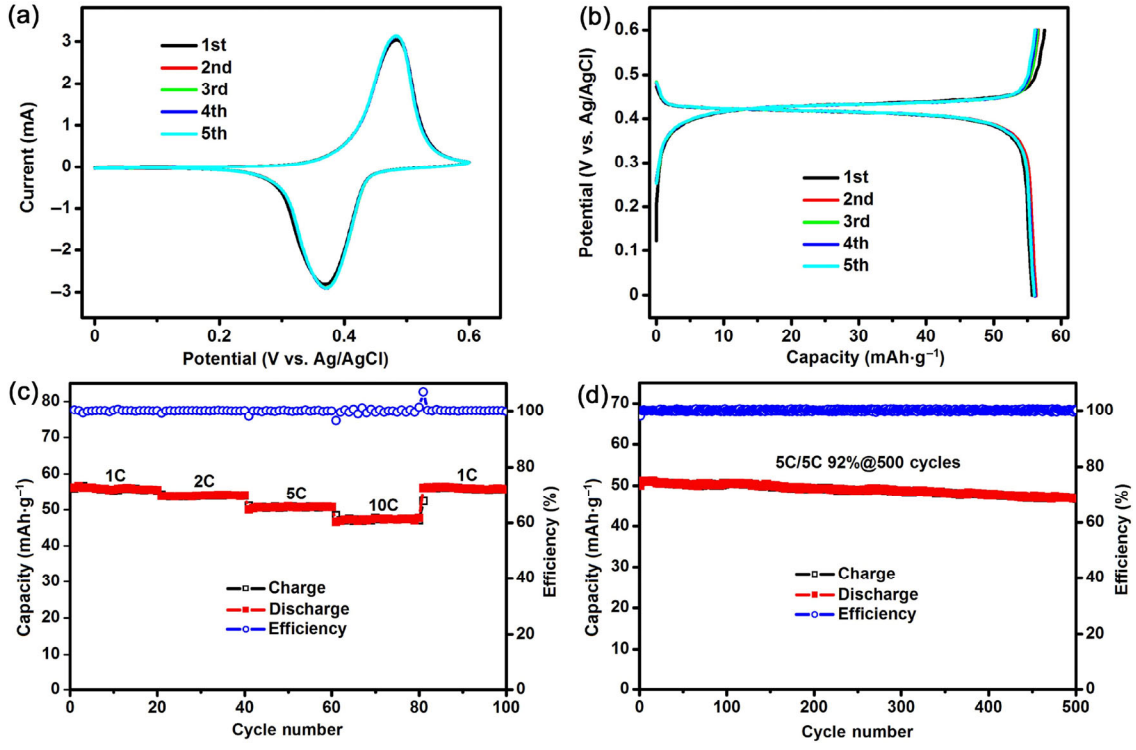

Figure 3 Electrochemical performance of $Na_2VTi(PO_4)_3$ electrode as the cathode in a three electrode system in aqueous media. (a) Cyclic voltammograms measured between 0 V and 0.6 V at a scan rate of 0.5 $mV·s^{-1}$. (b) Typical charge/discharge profiles in the voltage of 0−0.6 V at a rate of 1C. (c) Rate capabilities at different rates from 1C to 10C. (d) The corresponding cycling performance with Coulombic efficiency over 500 cycles at a rate of 5C.

recover to their original states on discharging to 0 V (Fig. S2 in the ESM). The $Na_2VTi(PO_4)_3$ electrode exhibits similar charge and discharge profiles with well-defined voltage plateaus and little polarization, indicating the reversibility of $Na_2VTi(PO_4)_3$ during successive charge/discharge cycles through the V^{4+}/V^{3+} redox couple. The high-rate capability and cycling stability of the $Na_2VTi(PO_4)_3$ electrode are displayed in Fig. 3(c). The reversible capacity of $Na_2VTi(PO_4)_3$ electrode slightly decreases from 56 $mAh·g^{-1}$ to 51 $mAh·g^{-1}$ when the current rate increases from 1C to 5C, while the Coulombic efficiency remains at ~100% at various rates. Even at a high rate of 10C, the electrode exhibits a reversible capacity of ~47 $mAh·g^{-1}$. The $Na_2VTi(PO_4)_3$ electrode was cycled at 5C with a slight capacity decay up to 500 cycles as shown in Fig. 3(d). The high-rate cyclability is attributed to the carbon coating that improves the electrical conductivity and the substitution of Ti that enhances the structure stability for the $Na_2VTi(PO_4)_3$ material in aqueous media [23, 31].

The electrochemical properties of the $Na_2VTi(PO_4)_3$ electrode when used as an anode were evaluated in a three electrode system in aqueous Na_2SO_4 electrolyte, as shown in Fig. 4. A pair of symmetric redox peaks at –0.80 V and –0.71 V is obtained for the $Na_2VTi(PO_4)_3$ anode (Fig. 4(a)), corresponding to the reversible insertion/extraction reaction of sodium ions into/from the $Na_2VTi(PO_4)_3$ lattice as in Eq. (2):

$$Na_2VTi(PO_4)_3 + xNa^+ + xe^- \rightleftharpoons Na_{2+x}VTi(PO_4)_3 \quad (2)$$

The obtained voltage of the Ti^{4+}/Ti^{3+} redox couple in $Na_2VTi(PO_4)_3$ is in agreement with that of the Ti^{4+}/Ti^{3+} redox couple in $NaTi_2(PO_4)_3$ [32–34]. The $Na_2VTi(PO_4)_3$ anode exhibits a reversible desodiation capacity of ~51 $mAh·g^{-1}$ and the Coulombic efficiency remains stable at 85% after the second cycle at 1C (Fig. 4(b)). When cycled at 5C, the discharge/charge Coulombic efficiency of $Na_2VTi(PO_4)_3$ in the aqueous electrolyte is 96%. This discrepancy becomes more obscure on cycling $Na_2VTi(PO_4)_3$ at 10C with a Coulombic efficiency of 98% (Fig. 4(c)). This is because

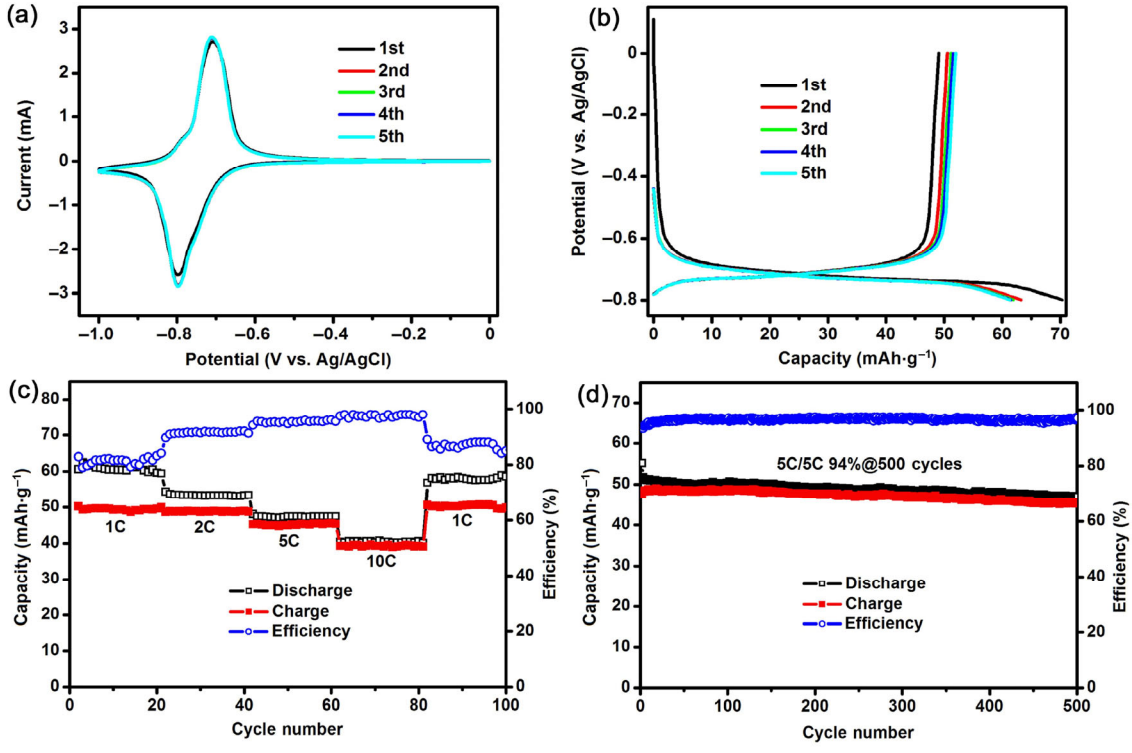

Figure 4 The electrochemical performance of $Na_2VTi(PO_4)_3$ electrode as anode in a three electrode system in aqueous media. (a) Cyclic voltammograms between −1.0 V and 0 V at a scan rate of 0.5 mV·s^{-1}. (b) Typical discharge/charge profiles in the voltage of −0.8–0 V at a rate of 1C. (c) Rate capabilities at different rates from 1C to 10C. (d) The corresponding cycling performance with Coulombic efficiency over 500 cycles at a rate of 5C.

the reduction state $Na_{2+x}VTi(PO_4)_3$ is chemically oxidized to $Na_2VTi(PO_4)_3$ by the dissolved O_2 in the aqueous electrolyte during the discharging of $Na_2VTi(PO_4)_3$ with a low current rate (Fig. S3 in the ESM), while the $Na_2VTi(PO_4)_3$ electrode undergoes electrochemical reduction on discharging at a high current rate [35]. However, the $Na_2VTi(PO_4)_3$ electrode was cycled well at 5C with a negligible capacity decay up to 500 cycles, as shown in Fig. 4(d). The excellent cyclability is attributed to the stable 3D framework of the NASICON structure that facilitates the reversible insertion/extraction of sodium ions without causing any structural change of the $Na_2VTi(PO_4)_3$ anode (Fig. S4 in the ESM).

Based on the above results, we initially demonstrated the fabrication of a battery of 1.2 V using $Na_2VTi(PO_4)_3$ with the redox couples of V^{4+}/V^{3+} and Ti^{4+}/Ti^{3+}, which are within the steady electrochemical window of water as shown in Fig. S5 (in the ESM). Subsequently, we assembled a symmetric NIB with a cathode-limited cell design using $Na_2VTi(PO_4)_3$ as both the cathode and anode materials. Fig. 5(a) demonstrates the CV curves of the symmetric cell between 0 and 1.8 V in aqueous electrolyte. The CV profiles of the initial five cycles overlap very well, and the oxidation and reduction peaks centered at 1.24 and 1.07 V are in consistent with the voltage differences between the V^{4+}/V^{3+} and Ti^{4+}/Ti^{3+} redox couples in the $Na_2VTi(PO_4)_3$ lattice. Unexpected oxidation and reduction peaks are observed beyond the voltage window of 0.2–1.5 V. Hence, we performed galvanostatic charge/discharge tests within the voltage window of 0.2–1.5 V in the full cell. The symmetric cell exhibits a charge plateau at 1.17 V and a discharge plateau at 1.14 V without any significant voltage hysteresis achieved at a rate of 1C as shown in Fig. 5(b), which is in good agreement with the CV data. Based on the mass of the active material in the cathode, the cell exhibits a reversible capacity of ~50 mAh·g^{-1}. A relatively low initial Coulombic efficiency of 79.4% is achieved; however, it increases up to 98% after the third cycle. The Coulombic efficiency of the full cell in the initial cycle

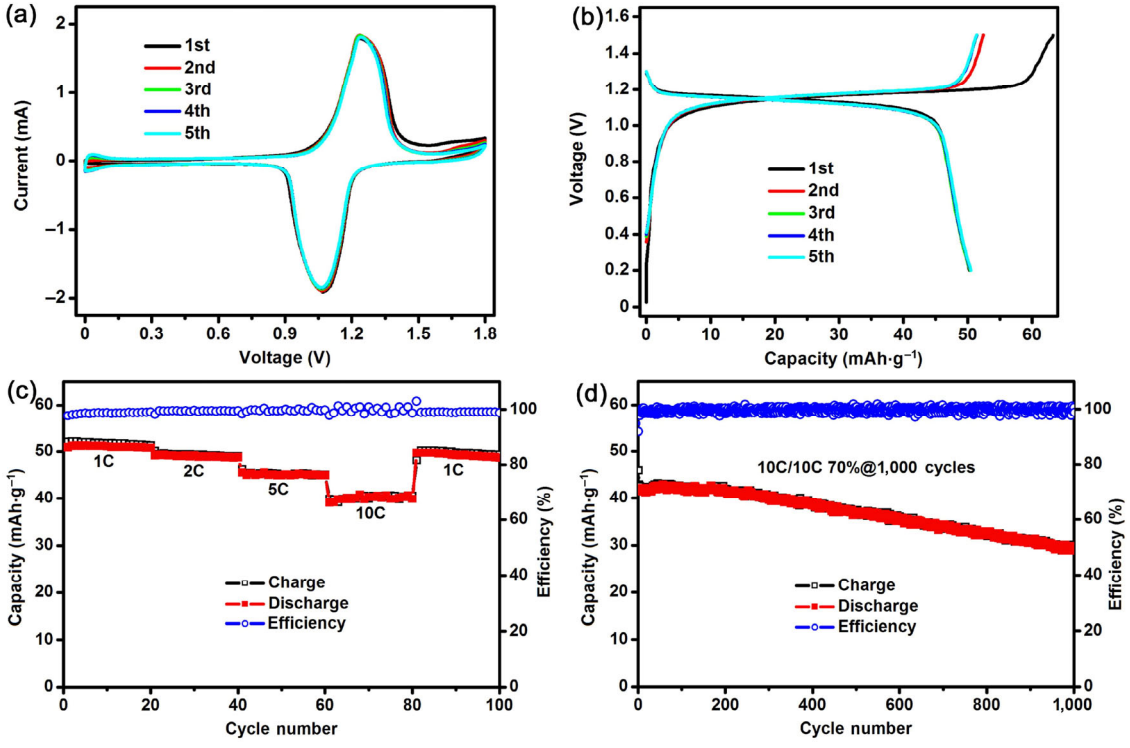

Figure 5 The electrochemical performance of the symmetric NIB with $Na_2VTi(PO_4)_3$ as both the cathode and anode in an aqueous electrolyte. (a) The cyclic voltammograms between 0 and 1.8 V at a scan rate of 0.5 $mV \cdot s^{-1}$. (b) Typical charge-discharge profiles in the voltage range of 0.2–1.5 V at a rate of 1C. (c) Rate capabilities at different rates from 1C to 10C. (d) The corresponding cycling performance with Coulombic efficiency over 1,000 cycles at a rate of 10C.

is closely related to the mass ratio and the Coulombic efficiency of the cathode and the anode. The energy density of the symmetric cell is ~30 $Wh \cdot kg^{-1}$ as calculated on the basis of the total mass of cathode and anode, which is comparable to or higher than that obtained for the recently developed aqueous asymmetric NIBs [36–39]. The rate capabilities of the symmetric cell were evaluated at various rates from 1C to 10C. As shown in Fig. 5(c), the reversible capacities of the cell are 50.4 $mAh \cdot g^{-1}$ at the rate of 1C and 40.6 $mAh \cdot g^{-1}$ at 10C, respectively. On further reducing the rate to 1C, a capacity of 49.7 $mAh \cdot g^{-1}$ is achieved, demonstrating the excellent rate capability of the symmetric cell. Fig. 5(d) shows that ~70% of the initial capacity is retained for the symmetric cell after 1,000 cycles at the rate of 10C and the Coulombic efficiency exceeded 99% in the charge/discharge process. This long-term cyclability is impressive, revealing the potential applications of NASICON-structured $Na_2VTi(PO_4)_3$ as a bi-functional electrode material in aqueous symmetric NIBs for stationary power stations.

4 Conclusions

In conclusion, a symmetric aqueous NIB is fabricated using a bi-functional electrode material, $Na_2VTi(PO_4)_3$. The full cell exhibits an energy density of ~30 $Wh \cdot kg^{-1}$ as calculated based on the mass of the cathode and the anode at 1C, and exhibits 70% capacity retention over 1,000 cycles at a high charge/discharge rate of 10C. These results confirm our strategy that high-safety, long-life, and low-cost stationary battery systems can be obtained using a single active material in an aqueous electrolyte. This study is expected to inspire the battery research community to explore novel bi-functional electrode materials for large-scale stationary energy storage applications in the near future.

Acknowledgements

This work was financially supported by Chinese government under the "Thousand Youth Talents Program", Zhejiang Province Science Fund for

Distinguished Young Scholars (No. LR16B060001), and Key Technology and Supporting Platform of Genetic Engineering of Materials under State's Key Project of Research and Development Plan (No. 2016YFB0700600).

Electronic Supplementary Material: Supplementary material (crystallographic and EDS data, XPS and *ex-situ* XRD analysis, cyclic voltammetry and linear sweep voltammetry tests) is available in the online version of this article at https://doi.org/10.1007/s12274-017-1657-5.

References

[1] Larcher, D.; Tarascon, J. M. Towards greener and more sustainable batteries for electrical energy storage. *Nat. Chem.* **2015**, *7*, 19–29.

[2] Lu, J.; Chen, Z. H.; Ma, Z. F.; Fan, F.; Curtiss, L. A.; Amine, K. The role of nanotechnology in the development of battery materials for electric vehicles. *Nat. Nanotechnol.* **2016**, *11*, 1031–1038.

[3] Kim, S. W.; Seo, D. H.; Ma, X. H.; Ceder, G.; Kang, K. Electrode materials for rechargeable sodium-ion batteries: Potential alternatives to current lithium-ion batteries. *Adv. Energy Mater.* **2012**, *2*, 710–721.

[4] Kundu, D.; Talaie, E.; Duffort, V.; Nazar, L. F. The emerging chemistry of sodium ion batteries for electrochemical energy storage. *Angew. Chem., Int. Ed.* **2015**, *54*, 3431–3448.

[5] Noguchi, Y.; Kobayashi, E.; Plashnitsa, L. S.; Okada, S.; Yamaki, J. I. Fabrication and performances of all solid-state symmetric sodium battery based on NASICON-related compounds. *Electrochim. Acta* **2013**, *101*, 59–65.

[6] Wang, S. W.; Wang, L. J.; Zhu, Z. Q.; Hu, Z.; Zhao, Q.; Chen, J. All organic sodium-ion batteries with $Na_4C_8H_2O_6$. *Angew. Chem., Int. Ed.* **2014**, *53*, 5892–5896.

[7] Shanmugam, R.; Lai, W. $Na_{2/3}Ni_{1/3}Ti_{2/3}O_2$: "Bi-functional" electrode materials for Na-ion batteries. *ECS Electrochem. Lett.* **2014**, *3*, A23–A25.

[8] Zhang, L.; Dou, S. X.; Liu, H. K; Huang, Y. H.; Hu, X. L. Symmetric electrodes for electrochemical energy-storage devices. *Adv. Sci.* **2016**, *3*, 1600115.

[9] Wang, Y. S.; Xiao, R. J.; Hu, Y. S.; Avdeev, M.; Chen, L. Q. P2-$Na_{0.6}[Cr_{0.6}Ti_{0.4}]O_2$ cation-disordered electrode for high-rate symmetric rechargeable sodium-ion batteries. *Nat. Commun.* **2015**, *6*, 6954.

[10] Guo, S. H.; Yu, H. J.; Liu, P.; Ren, Y.; Zhang, T.; Chen, M. W.; Ishida, M.; Zhou, H. S. High-performance symmetric sodium-ion batteries using a new, bipolar O3-type material, $Na_{0.8}Ni_{0.4}Ti_{0.6}O_2$. *Energy Environ. Sci.* **2015**, *8*, 1237–1244.

[11] Kim, H.; Hong, J.; Park, K. Y.; Kim, H.; Kim, S. W.; Kang, K. Aqueous rechargeable Li and Na ion batteries. *Chem. Rev.* **2014**, *114*, 11788–11827.

[12] You, Y.; Sang, Z. S.; Liu, J. P. Recent developments on aqueous sodium-ion batteries. *Mater. Technol.* **2016**, *31*, 501–509.

[13] Dong, X. L.; Chen, L.; Liu, J. Y.; Haller, S.; Wang, Y. G.; Xia, Y. Y. Environmentally-friendly aqueous Li (or Na)-ion battery with fast electrode kinetics and super-long life. *Sci. Adv.* **2016**, *2*, e1501038.

[14] Wu, X. Y.; Sun, M. Y.; Shen, Y. F.; Qian, J. F.; Cao, Y. L.; Ai, X. P.; Yang, H. X. Energetic aqueous rechargeable sodium-ion battery based on $Na_2CuFe(CN)_6$-$NaTi_2(PO_4)_3$ intercalation chemistry. *ChemSusChem* **2014**, *7*, 407–411.

[15] Gao, H. C; Goodenough, J. B. An aqueous symmetric sodium-ion battery with NASICON-structured $Na_3MnTi(PO_4)_3$. *Angew. Chem., Int. Ed.* **2016**, *55*, 12768–12772.

[16] Zhang, Q.; Liao, C. Y.; Zhai, T. Y.; Li, H. Q. A high rate 1.2 V aqueous sodium-ion battery based on all NASICON structured $NaTi_2(PO_4)_3$ and $Na_3V_2(PO_4)_3$. *Electrochim. Acta* **2016**, *196*, 470–478.

[17] Zhu, C. B.; Song, K. P.; van Aken, P. A.; Maier, J.; Yu, Y. Carbon-coated $Na_3V_2(PO_4)_3$ embedded in porous carbon matrix: An ultrafast Na-storage cathode with the potential of outperforming Li cathodes. *Nano Lett.* **2014**, *14*, 2175–2180.

[18] Liu, T. F.; Wang, B.; Gu, X. X.; Wang, L.; Ling, M.; Liu, G.; Wang, D. L.; Zhang, S. Q. All-climate sodium ion batteries based on the NASICON electrode materials. *Nano Energy* **2016**, *30*, 756–761.

[19] Park, S. I.; Gocheva, I.; Okada, S.; Yamaki, J. I. Electrochemical properties of $NaTi_2(PO_4)_3$ anode for rechargeable aqueous sodium-ion batteries. *J. Electrochem. Soc.* **2011**, *158*, A1067–A1070.

[20] Chen, L.; Shao, H. Z.; Zhou, X. F.; Liu, G. Q.; Jiang, J.; Liu, Z. P. Water-mediated cation intercalation of open-framework indium hexacyanoferrate with high voltage and fast kinetics. *Nat. Commun.* **2016**, *7*, 11982.

[21] Song, W. X.; Ji, X. B.; Zhu, Y. R.; Zhu, H. J.; Li, F. Q.; Chen, J.; Lu, F.; Yao, Y. P.; Banks, C. E. Aqueous sodium-ion battery using a $Na_3V_2(PO_4)_3$ electrode. *ChemElectroChem* **2014**, *1*, 871–876.

[22] Zhang, L. D.; Huang, T.; Yu, A. S. Carbon-coated $Na_3V_2(PO_4)_3$ nanocomposite as a novel high rate cathode material for aqueous sodium ion batteries. *J. Alloys Compd.* **2015**, *646*, 522–527.

[23] Mason, C. W.; Lange, F. Aqueous ion battery systems using sodium vanadium phosphate stabilized by titanium substitution. *ECS Electrochem. Lett.* **2015**, *4*, A79–A82.

[24] Liu, J.; Zhang, J. G.; Yang, Z. G.; Lemmon, J. P.; Imhoff, C.; Graff, G. L.; Li, L. Y.; Hu, J. Z.; Wang, C. M.; Xiao, J. et al. Materials science and materials chemistry for large scale electrochemical energy storage: From transportation to electrical grid. *Adv. Funct. Mater.* **2013**, *23*, 929–946.

[25] Guo, S. H.; Liu, P.; Sun, Y.; Zhu, K.; Yi, J.; Chen, M. W.; Ishida, M.; Zhou, H. S. A high-voltage and ultralong-life sodium full cell for stationary energy storage. *Angew. Chem., Int. Ed.* **2015**, *54*, 11701–11705.

[26] Song, W. X.; Cao, X. Y.; Wu, Z. P.; Chen, J.; Huangfu, K. L.; Wang, X. W.; Huang, Y. L.; Ji, X. B.A study into the extracted ion number for NASICON structured $Na_3V_2(PO_4)_3$ in sodium-ion batteries. *Phys. Chem. Chem. Phys.* **2014**, *16*, 17681–17687.

[27] Jian, Z. L.; Zhao, L.; Pan, H. L.; Hu, Y.-S.; Li, H.; Chen, W.; Chen, L. Q. Carbon coated $Na_3V_2(PO_4)_3$ as novel electrode material for sodium ion batteries. *Electrochem. Commun.* **2012**, *14*, 86–89.

[28] Shen, W.; Wang, C.; Liu, H. M.; Yang, W. S. Towards highly stable storage of sodium ions: A porous $Na_3V_2(PO_4)_3$/C cathode material for sodium-ion batteries. *Chemistry* **2013**, *19*, 14712–14718.

[29] Kumar, P. R.; Jung, Y. H.; Lim, C. H.; Kim, D. K. $Na_3V_2O_{2x}(PO_4)_2F_{3-2x}$: A stable and high-voltage cathode material for aqueous sodium-ion batteries with high energy density. *J. Mater. Chem. A* **2015**, *3*, 6271–6275.

[30] Lim, S. Y.; Kim, H.; Shakoor, R. A.; Jung, Y.; Choi, J. W. Electrochemical and thermal properties of NASICON structured $Na_3V_2(PO_4)_3$ as a sodium rechargeable battery cathode: A combined experimental and theoretical study. *J. Electrochem. Soc.* **2012**, *159*, A1393–A1397.

[31] Li, S.; Dong, Y. F.; Xu, L.; Xu, X.; He, L.; Mai, L. Q. Effect of carbon matrix dimensions on the electrochemical properties of $Na_3V_2(PO_4)_3$Nanograins for high-performance symmetric sodium-ion batteries. *Adv. Mater.* **2014**, *26*, 3545–3553.

[32] Vujković, M.; Mitrić, M.; Mentus, S. High-rate intercalation capability of $NaTi_2(PO_4)_3$/C composite in aqueous lithium and sodium nitrate solutions. *J. Power Sources* **2015**, *288*, 176–186.

[33] Roh, H. K.; Kim, H. K.; Kim, M. S.; Kim, D. H.; Chung, K. Y.; Roh, K. C.; Kim, K. B. *In situ* synthesis of chemically bonded $NaTi_2(PO_4)_3$/rGO 2D nanocomposite for high-rate sodium-ion batteries. *Nano Res.* **2016**, *9*, 1844–1855.

[34] Song, J. J.; Park, S.; Gim, J.; Mathew, V.; Kim, S.; Jo, J.; Kim, S.; Kim, J. High rate performance of a $NaTi_2(PO_4)_3$/rGO composite electrode via pyro synthesis for sodium ion batteries. *J. Mater. Chem. A* **2016**, *4*, 7815–7822.

[35] Luo, J. Y.; Cui, W. J.; He, P.; Xia, Y. Y. Raising the cycling stability of aqueous lithium-ion batteries by eliminating oxygen in the electrolyte. *Nat. Chem.* **2010**, *2*, 760–765.

[36] Hou, Z. G.; Li, X. N.; Liang, J. W.; Zhu, Y. C.; Qian, Y. T. An aqueous rechargeable sodium ion battery based on a $NaMnO_2$-$NaTi_2(PO_4)_3$ hybrid system for stationary energy storage. *J. Mater. Chem. A* **2015**, *3*, 1400–1404.

[37] Li, Z.; Young, D.; Xiang, K.; Carter, W. C.; Chiang, Y. M. Towards high power high energy aqueous sodium-ion batteries: The $NaTi_2(PO_4)_3$/$Na_{0.44}MnO_2$system. *Adv. Energy Mater.* **2013**, *3*, 290–294.

[38] Pasta, M.; Wessells, C. D.; Liu, N.; Nelson, J.; McDowell, M. T.; Huggins, R. A.; Toney, M. F.; Cui, Y. Full open-framework batteries for stationary energy storage. *Nat. Commun.* **2014**, *5*, 3007.

[39] Liu, Y.; Zhang, B. H.; Xiao, S. Y.; Liu, L. L.; Wen, Z. B.; Wu, Y. P. A nanocomposite of MoO_3 coated with PPy as an anode material for aqueous sodium rechargeable batteries with excellent electrochemical performance. *Electrochim. Acta* **2014**, *116*, 512–517.